Geoderma 259–260 (2015) 288–299

Contents lists available at ScienceDirect

Geoderma

journal homepage: www.elsevier.com/locate/geoderma

Impact of alley cropping agroforestry on stocks, forms and spatial distribution of soil organic carbon — A case study in a Mediterranean context

Rémi Cardinael [a,d], Tiphaine Chevallier [a,*], Bernard G. Barthès [a], Nicolas P.A. Saby [b], Théophile Parent [a], Christian Dupraz [c], Martial Bernoux [a], Claire Chenu [d]

[a] IRD, UMR 210 Eco&Sols, Montpellier SupAgro, 34060 Montpellier, France
[b] INRA, US 1106 Infosol, F 45075 Orléans, France
[c] INRA, UMR 1230 System, Montpellier SupAgro, 34060 Montpellier, France
[d] AgroParisTech, UMR 1402 Ecosys, Avenue Lucien Brétignières, 78850 Thiverval-Grignon, France

ARTICLE INFO

Article history:
Received 27 February 2015
Received in revised form 16 June 2015
Accepted 17 June 2015
Available online xxxx

Keywords:
Soil mapping
Soil organic carbon storage
Soil organic carbon saturation
Deep soil organic carbon stocks
Visible and near infrared spectroscopy
Particle-size fractionation

ABSTRACT

Agroforestry systems, i.e., agroecosystems combining trees with farming practices, are of particular interest as they combine the potential to increase biomass and soil carbon (C) storage while maintaining an agricultural production. However, most present knowledge on the impact of agroforestry systems on soil organic carbon (SOC) storage comes from tropical systems. This study was conducted in southern France, in an 18-year-old agroforestry plot, where hybrid walnuts (*Juglans regia* × *nigra* L.) are intercropped with durum wheat (*Triticum turgidum* L. subsp. *durum*), and in an adjacent agricultural control plot, where durum wheat is the sole crop. We quantified SOC stocks to 2.0 m depth and their spatial variability in relation to the distance to the trees and to the tree rows. The distribution of additional SOC storage in different soil particle-size fractions was also characterized. SOC accumulation rates between the agroforestry and the agricultural plots were 248 ± 31 kg C ha^{-1} yr^{-1} for an equivalent soil mass (ESM) of 4000 Mg ha^{-1} (to 26–29 cm depth) and 350 ± 41 kg C ha^{-1} yr^{-1} for an ESM of 15,700 Mg ha^{-1} (to 93–98 cm depth). SOC stocks were higher in the tree rows where herbaceous vegetation grew and where the soil was not tilled, but no effect of the distance to the trees (0 to 10 m) on SOC stocks was observed. Most of the additional SOC storage was found in coarse organic fractions (50–200 and 200–2000 μm), which may be rather labile fractions. All together our study demonstrated the potential of alley cropping agroforestry systems under Mediterranean conditions to store SOC, and questioned the stability of this storage.

1. Introduction

Agroforestry systems are defined as agroecosystems associating trees with farming practices (Somarriba, 1992; Torquebiau, 2000). Several types of agroforestry systems can be distinguished depending on the different associations of trees, crops and animals (Torquebiau, 2000). In temperate regions, an important part of recently established agroforestry systems is alley cropping systems, where parallel tree rows are planted in crop lands, and designed to allow mechanization of annual crops. Agroforestry systems are of particular interest as they combine the potential to provide a variety of non-marketed ecosystem services, defined as the benefits people obtain from ecosystems (Millennium Ecosystem Assessment, 2005; Power, 2010) while maintaining a high agricultural production (Clough et al., 2011). For instance, agroforestry systems can contribute to water quality improvement (Bergeron et al., 2011; Tully et al., 2012), biodiversity enhancement (Schroth et al., 2004; Varah et al., 2013), and erosion control (Young, 1997). But agroforestry systems are also increasingly recognized as a useful tool to help mitigate global warming (Pandey, 2002; Stavi and Lal, 2013; Verchot et al., 2007). Trees associated to annual crops store the carbon (C) assimilated through photosynthesis into their aboveground and belowground biomass. The residence time of C in the harvested biomass will depend on the fate of woody products, and can reach many decades especially for timber wood (Bauhus et al., 2010; Profft et al., 2009). Agroforestry trees also produce organic matter (OM) inputs to the soil (Jordan, 2004; Peichl et al., 2006), and could thus enhance soil organic carbon (SOC) stocks. Leaf litter and pruning residues are left on the soil, whereas OM originating from root mortality and root exudates can be incorporated much deeper into the soil as agroforestry trees may have a very deep rooting to minimize the competition with the annual crop (Cardinael et al., 2015; Mulia and Dupraz, 2006). Moreover, several studies showed that root-derived C was preferentially stabilized in soil compared to above ground derived C (Balesdent and Balabane, 1996; Rasse et al., 2005), mainly due to physical protection of root hairs within soil aggregates (Gale et al., 2000), to chemical recalcitrance of root components (Bird and Torn, 2006), or to

* Corresponding author.
E-mail address: tiphaine.chevallier@ird.fr (T. Chevallier).

http://dx.doi.org/10.1016/j.geoderma.2015.06.015
0016-7061/

adsorption of root exudates or decomposition products on clay particles (Chenu and Plante, 2006; Oades, 1995). Compared to an agricultural field, additional inputs of C from tree roots could therefore be stored deep into the soil, but could also enhance decomposition of SOM, i.e., due to the priming effect (Fontaine et al., 2007).

Although it is generally assumed that agroforestry system has the potential to increase SOC stocks (Lorenz and Lal, 2014), quantitative estimates are scarce, especially for temperate (Nair et al., 2010; Peichl et al., 2006; Pellerin et al., 2013; Upson and Burgess, 2013) or Mediterranean (Howlett et al., 2011) agroforestry systems combining crops and tree rows. Most studies concern tropical regions where agroforestry is a more widespread agricultural practice (Albrecht and Kandji, 2003; Somarriba et al., 2013).

Moreover, as pointed out by Nair (2012), very few studies assessed the impact of agroforestry trees deep in the soil (Haile et al., 2010; Howlett et al., 2011; Upson and Burgess, 2013). Most of them considered SOC at depths above 0.5 m (Bambrick et al., 2010; Oelbermann and Voroney, 2007; Oelbermann et al., 2004; Peichl et al., 2006; Sharrow and Ismail, 2004). This lack of knowledge concerning deep soil is mainly due to difficulties to attain profound soil depths, and to the cost of analyzing soil samples from several soil layers. Recently, new methods such as visible and near infrared reflectance (VNIR) spectroscopy have been developed (Brown et al., 2006; Stevens et al., 2013). They allow time- and cost-effective determination of SOC concentration, in the laboratory but also in the field (Gras et al., 2014). Additionally to the lack of data for deep soil, reference plots were not always available, preventing from estimating the additional storage of SOC due specifically to agroforestry (Howlett et al., 2011).

In alley cropping systems, spaces between trees in tree rows are usually covered by natural or sowed herbaceous vegetation, and the soil under tree rows is usually not tilled, which may favor SOC storage in soil (Virto et al., 2011). Moreover, while trees strongly affect the depth and spatial distribution of OM inputs to soils (Rhoades, 1997), distribution of SOC stocks close and away from trees was seldom considered. Some authors reported higher SOC stocks under the tree canopy than 5 m from the tree to 1 m soil depth (Howlett et al., 2011), others found that spatial distribution of SOC stocks could vary with the age of the trees (Bambrick et al., 2010). Some authors reported that spatial distribution of SOC stocks to 20 cm depth was not explained by the distance to the trees but by the design of the agroforestry system, tree rows having higher SOC stocks than inter-rows whatever the distance to the trees (Peichl et al., 2006; Upson and Burgess, 2013). To our knowledge, geostatistical methods (Webster and Oliver, 2007) have never been used to describe the spatial distribution of SOC stocks in alley cropping agroforestry system although they have been recognized to be very powerful to map and understand spatial heterogeneity at the plot scale (Philippot et al., 2009) especially when dealing with more diverse and heterogeneous systems.

In addition, it is not known whether additional SOC (compared to an agricultural field) due to the presence of trees and tree rows, corresponds to soil fractions with a rapid turnover, such as particulate organic matter (POM), or to clay and silt associated OM, likely to be stabilized in soil for a longer period of time (Balesdent et al., 1998). Takimoto et al. (2008) and Howlett et al. (2011) found that carbon content of coarse organic fractions was increased at different depths under agroforestry systems. But, Haile et al. (2010) found that trees grown in a silvopastoral system contributed to most of the SOC associated to the fine silt + clay fractions to 1 m depth. The potential of a soil for SOC storage in a stable form is limited by the amount of fine particles (clay + fine silt) and can be estimated by the difference between the theoretical SOC saturation (Hassink, 1997) and the measured SOC saturation value for the fine fraction (Angers et al., 2011; Wiesmeier et al., 2014).

In this study, we aimed to assess the effect of introducing rows of timber trees into arable land on SOC storage. For this i) we quantified SOC stocks to a depth of 2.0 m in an agroforestry plot and in an adjacent agricultural control plot, ii) we assessed the spatial distribution of SOC stocks in a geostatistical framework taking into account the distance to the trees and to the tree rows, and iii) we studied the distribution of SOC in different soil particle-size fractions.

We hypothesized that SOC stocks would be higher in the agroforestry plot compared to the control plot, also at depth, and that SOC stocks would decrease with increasing distance to the trees at all depths. Moreover, our hypothesis was that additional SOC in the agroforestry plot compared to the control plot would enrich all particle-size fractions.

2. Materials and methods

2.1. Site description

The experimental site was located in Prades-le-Lez, 15 km North of Montpellier, France (Longitude 04°01′ E, Latitude 43°43′ N, elevation 54 m a.s.l.). The climate is sub-humid Mediterranean with an average temperature of 15. 4°C and an average annual rainfall of 873 mm (years 1995–2013). The soil is a silty and carbonated deep alluvial Fluvisol (IUSS Working Group WRB, 2007). From 1950 to 1960, the site was a vineyard (*Vitis vinifera* L.), and from 1960 to 1985 the field was occupied by an apple (*Malus* Mill.) orchard. The apple tree stumps were removed in 1985. Then, durum wheat (*Triticum turgidum* L. subsp. *durum* (Desf.) Husn.) was cultivated. In February 1995, a 4.6 ha agroforestry alley-cropping plot was established after the soil was plowed to 20 cm depth, with the planting of hybrid walnuts (*Juglans regia* × *nigra* cv. NG23) at 13 × 4 m spacing, with East–West tree rows (Fig. 1). The remaining part of the plot (1.4 ha) was kept as a control agricultural plot. The walnut trees were planted at an initial density of 200 trees ha^{-1}. They were thinned in 2004 down to 110 trees ha^{-1}. In the tree rows, the soil was not tilled and spontaneous herbaceous vegetation grew. The cultivated inter-row was 11 m wide. Since the tree planting, the agroforestry inter-row and the control plot were managed in the same way. The annual crop was most of the time durum wheat, except in 1998, 2001 and 2006, when rapeseed (*Brassica napus* L.) was cultivated, and in 2010 and 2013, when pea (*Pisum sativum* L.) was cultivated. The durum wheat crop was fertilized as a conventional crop (120 kg N ha^{-1} yr^{-1}), and the soil was plowed annually to 20 cm depth, before durum wheat was sown.

2.2. Soil core sampling

The experimental site was not designed as traditional agronomical experiments with blocks and replicates, but with two large adjacent plots. First, soil texture was analyzed for 24 profiles down to 2 m soil depth, following a random sampling design within the two plots. In May 2013, a sub-plot of 625 m^2 was sampled in both plots, following an intensive sampling scheme (Fig. 2). In the agroforestry plot, this sub-plot included two tree rows, two inter-rows and nine walnut trees. Walnut trees had a mean height of 11.21 ± 0.65 m, a mean height of merchantable timber of 4.49 ± 0.39 m and a mean diameter at breast height of 25.54 ± 1.36 cm. Soil cores (n = 36) were sampled on a regular grid, every 5 m (Fig. 2). Around each tree, a soil core was collected at 1 m, 2 m and 3 m distance from the tree (n = 57), in the tree row and perpendicular to the tree row. Seven soil cores were sampled additionally in the middle of the inter-row to study short scale (1 m distance) spatial heterogeneity of SOC stocks far from the trees (Fig. 2). The same sampling scheme was followed in the control plot without these seven additional soil cores. Thus, 100 soil cores were sampled in the agroforestry sub-plot (40 in tree rows, 60 in inter-rows) and 93 in the agricultural sub-plot (Fig. 2). All cores were sampled down to 2 m depth using a motor-driven micro caterpillar driller (8.5-cm diameter and 1-m long soil probe). The soil probe was successively pushed two times into the soil, to get 0–1 m and 1–2 m cores at each sampling point. Each soil core was then cut into ten segments, corresponding to the following depth increments: 0–10, 10–30, 30–50, 50–70, 70–100, 100–120, 120–140, 140–160, 160–180, and 180–200 cm.

Fig. 1. Hybrid walnut–durum wheat agroforestry system. Left panel: in November 2013; Right panel: in June 2014.

2.3. Use of field visible and near infrared spectroscopy to predict SOC

As core surface had been smoothed by the soil probe, each segment was refreshed with a knife before being scanned, in order to provide a plane but un-smoothed surface. Then, four VNIR spectra (from 350 to 2500 nm at 1 nm increment) were acquired in the field at different places of each segment, using a portable spectrophotometer ASD LabSpec 2500 (Analytical Spectral Devices, Boulder, CO, USA), and were then averaged. Reflectance spectra were recorded as absorbance, which is the logarithm of the inverse of reflectance. The whole spectrum population was composed of 1908 mean spectra (i.e. 193 cores with 10 segments per core but a few samples were lost due to mechanical problems). In topsoil (0–30 cm), the soil was dry and crumbled whereas in deeper soil horizons, it was moister and had higher cohesion. Thus, two different predictive models were built: one for topsoil samples, the other for subsoil (30–200 cm) samples. The "topsoil model" for predicting SOC was built using the 116 most representative topsoil samples, out of 380 samples, and the "subsoil model", using the 142 most representative subsoil samples, out of 1488 samples. The procedure to select the most representative samples is presented below. The 0–10 cm soil layer from the tree rows (40 samples) was not used for the topsoil model as it contained abundant plant debris <2 mm (roots, leaves, etc.) and a PCA revealed that these VNIR spectra were different from the whole spectra population. SOC concentration of these samples was therefore determined with a CHN elemental analyzer, and, thus, not predicted by VNIR. The SOC concentration of the 258 samples selected for building the VNIR prediction models was also analyzed using a CHN elemental analyzer.

2.4. VNIR spectra analysis and construction of predictive models

VNIR spectra analysis was conducted on topsoil and subsoil samples separately, using the WinISI 4 software (Foss NIRSystems/Tecator Infrasoft International, LLC, Silver Spring, MD, USA) and R software version 3.1.1 (R Development Core Team, 2013). The most representative samples, from a spectral viewpoint, were selected using the Kennard–Stone algorithm, which is based on distance calculation between sample spectra in the principal component space (Kennard and Stone, 1969). For the topsoil model, the calibration subset included 104 samples (90%) selected as the most representative spectrally, and the validation subset 12 samples (10%). For the subsoil model, the calibration subset included 128 samples (90%), and the validation subset 14 samples. Fitting the spectra to the SOC concentrations determined with a CHN elemental analyzer was performed using partial least squares regression (PLSR; Martens and Naes, 1989). We tested common spectrum preprocessing techniques including first and second derivatives, de-trending, standard normal variate transformation and multiplicative scatter correction, but the best models were obtained when no pre-treatment was applied on the spectra (data not shown). Then cross-validation was performed within the calibration subset, using groups that were randomly selected (10 groups), in order to build the model used for making predictions on the samples not analyzed in the laboratory. No outlier was removed. The number of components (latent variables) that minimized the standard error of cross-validation (SECV) was retained for the PLSR. The performance of the models was assessed on the validation subsets using the coefficient of determination (R^2) and the standard error of prediction (SEP) between predicted and measured

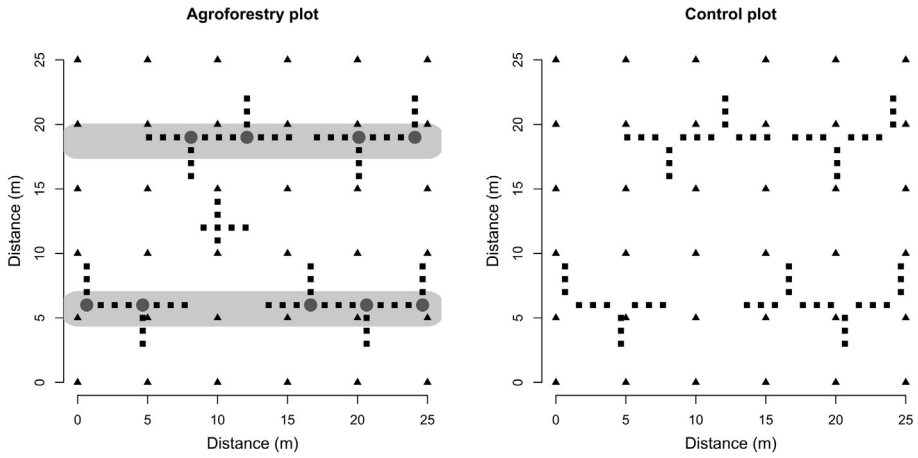

Fig. 2. Description of the intensive sampling scheme in the agroforestry and in the control sub-plots. Circles represent hybrid walnuts, the grey strips represent the tree rows, triangles are for soil cores on the regular grid (every 5 m), squares are for soil cores on transects (every 1 m).

values, and also the ratio of standard deviation to SEP, denoted RPD, and the RPIQ, which is the ratio of performance to IQ (interquartile distance), i.e. IQ/SEP = (Q3 − Q1)/SEP, where Q1 is the 25th percentile and Q3 is the 75th percentile (Bellon-Maurel et al., 2010). Then all subset samples (i.e., calibration and validation samples) were used to build models that were applied on the samples not analyzed in the laboratory. The performance of these models was also assessed according to R^2, SECV, RPD and RPIQ.

Subsoil models performed better than topsoil models (Table 1, Fig. S1). In external validation, RPD was higher than 2 for the subsoil, which has been considered a threshold for accurate NIRS prediction of soil properties in the laboratory (Chang et al., 2001). This RPD threshold was not achieved for the topsoil model, but SOC concentrations were predicted for less than 60% of topsoil samples, the rest was directly analyzed with a CHN elemental analyzer. It is worth noting that cross-validation on the whole set (for making prediction on the samples not analyzed in the lab) yielded better results than external validation (on 10% of analyzed samples) in the subsoil, but the opposite was observed in the topsoil.

2.5. Bulk densities determination

Each segment was weighed in the field to determine its humid mass. Following this step, each segment was crumbled and homogenized, and a representative sub-sample of about 300 g was sampled. Sub-samples were sieved at 2 mm to separate coarse fragments such as stones and living roots. Coarse fragments represented less than 1% of each soil mass and were considered as negligible. Moisture contents were determined for 23 soil cores (i.e. 230 samples) after 48 h drying at 105 °C, and were used to calculate the dry mass of all samples. Bulk density (BD) was determined for each sample by dividing the dry mass of soil by its volume in the soil corer tube.

2.6. Reference analysis measurements

After air drying, soil samples were oven dried at 40 °C for 48 h, sieved at 2 mm, and ball milled until they passed a 200 μm mesh sieve. Carbonates were removed by acid fumigation, following Harris et al. (2001). For this, 30 mg of soil was placed in open Ag-foil capsules. The capsules were then placed in the wells of a microtiter plate and 50 μL of demineralized water was added in each capsule. The microtiter plate was then placed in a vacuum desiccator with a beaker filled with 100 mL of concentrated HCl (37%). The samples were exposed to HCl vapors for 8 h, and were then dried at 60 °C for 48 h. Capsules were then closed in a bigger tin capsule. Decarbonated samples were analyzed for organic carbon concentration with a CHN elemental analyzer (Carlo Erba NA 2000, Milan, Italy). Isotopic measurements were performed on a few samples to check that decarbonation was well performed ($\delta^{13}C$ OM = −25‰).

2.7. Soil organic carbon stock calculation

In most studies comparing SOC stocks between treatments or over time periods, SOC stocks have been quantified to a fixed depth as the product of soil bulk density, depth and SOC concentration. However, if soil bulk density differs between the treatments being compared, the fixed-depth method has been shown to introduce errors (Ellert et al., 2002). A more accurate method is to use an equivalent soil mass (ESM) (Ellert and Bettany, 1995). We defined a reference soil mass profile that was used as the basis for comparison, based on the lowest soil mass observed at each sampling depth and location. For this reference, soil mass layers (0–1000, 1000–4000, 4000–7300, 7300–10700, 10700–15700, 15700–18700, 18700–21900, 21900–25100, 25100–28300, 28300–31500 Mg ha^{-1}) corresponded roughly to soil depth layers (0–10, 10–30, 30–50, 50–70, 70–100, 100–120, 120–140, 140–160, 160–180, 180–200 cm, respectively). For the different treatments (control, tree row, inter-row), SOC stocks were calculated on this basis, soil mass was the same, whereas depth layer varied (Table 2). The effect of the ESM correction can be seen in Table S1. SOC stocks in the agroforestry plot were calculated with tree rows representing 16% of the plot surface area and inter-rows 84%:

$$\text{SOC stock}_{Agroforestry} = 0.16 \times \text{SOC stock}_{Tree\ row} + 0.84 \times \text{SOC stock}_{Inter\ row}. \quad (1)$$

We defined delta SOC stock as the difference between SOC stock in the agroforestry plot and in the control plot:

$$\Delta\ \text{SOC stock} = \text{SOC stock}_{Agroforestry} - \text{SOC stock}_{Control}. \quad (2)$$

All SOC stocks were expressed in Mg C ha^{-1}. SOC accumulation rates (kg C ha^{-1} yr^{-1}) were calculated by dividing delta stocks by the number of years since the tree planting (18 years):

$$\text{SOC accumulation rate} = \frac{\Delta\ \text{SOC stock}}{18} \times 1000\ . \quad (3)$$

2.8. Particle-size fractionation

Particle-size fractionation was performed for five soil cores from the inter-rows, five from the tree rows and six from the control plot, and at four depths: 0–10, 10–30, 70–100 and 160–180 cm. Thus, 64 soil samples were fractionated, as described in Balesdent et al. (1998) and Gavinelli et al. (1995). Briefly, 20 g of 2-mm sieved samples were soaked overnight at 4 °C in 300 mL of deionized water, with 10 mL of sodium metaphosphate (HMP, 50 g L^{-1}). Samples were then shaken 2 h with 10 glass balls in a rotary shaker, at 43 rpm. The soil suspension was wet-sieved through 200-μm and 50-μm sieves, successively. The fractions remaining on the sieves were density-separated into organic fractions, floating in water, and remaining mineral fractions. The 0–50 μm suspension was ultrasonicated during 10 min with a probe-type ultrasound generating unit (Fisher Bioblock Scientific, Illkirch, France) having a power output of 600 W and working in 0.7:0.3 operating/interruption intervals. This 0–50 μm suspension was then sieved through a 20-μm sieve. The resulting 0–20 μm suspension was transferred to 1-L glass cylinders, which were then shaken by hand and 50 mL of the suspension were withdrawn immediately after. They

Table 1
External validation and prediction model results for soil organic carbon. N: numbers of samples; SD: standard deviation (mean and standard deviation of the conventional determinations); R^2: coefficient of determination; RPD is the ratio of performance to deviation, i.e. the ratio of SD to SEP or SECV. RPIQ is the ratio of performance to IQ (interquartile distance), i.e. IQ/SEP (or SECV) = (Q3 − Q1)/SEP (or SECV).

External validation on 10% samples after calibration using 90% samples								Prediction model using 100% samples (10-group cross-validation)						
N	Mean mg g^{-1}	SD mg g^{-1}	SEP mg g^{-1}	Bias mg g^{-1}	R^2	RPD	RPIQ	N	Mean mg g^{-1}	SD mg g^{-1}	SECV mg g^{-1}	R^2	RPD	RPIQ
Topsoil														
12	9.71	2.09	1.04	−0.59	0.78	1.75	2.60	116	9.18	1.99	1.20	0.63	1.66	4.35
Subsoil														
14	6.19	1.80	0.83	0.01	0.74	2.03	3.03	142	6.06	1.86	0.77	0.83	2.40	4.85

Table 2
Soil organic carbon stocks (Mg C ha^{-1}) and SOC accumulation rates (kg C ha^{-1} yr^{-1}). Associated errors are standard errors (40 replicates for the tree-row, 60 replicates for the inter-row, and 93 replicates for the control plot). ESM = Equivalent Soil Mass. Significantly (P-value < 0.05) different SOC stocks are followed by different letters.

Cumulated ESM (Mg ha^{-1})	Cumulated calculated depth to ESM (cm)			Cumulated SOC stocks (Mg C ha^{-1})				Δ SOC stocks (Mg C ha^{-1})	SOC accumulation rates (kg C ha^{-1} yr^{-1})	
	Tree-row	Inter-row	Control	Tree-row	Inter-row	Agroforestry	Control	Δ (Agroforestry − Control)	Agroforestry vs Control	Inter-row vs Control
1000	0–9	0–8	0–7	21.6 ± 1.0a	9.8 ± 0.4c	11.7 ± 0.3b	9.3 ± 0.1c	2.3 ± 0.4	129 ± 20	24 ± 21
4000	0–29	0–27	0–26	52.8 ± 1.4a	37.9 ± 0.6c	40.3 ± 0.5b	35.8 ± 0.2d	4.5 ± 0.6	248 ± 31	115 ± 33
7300	0–49	0–47	0–45	77.1 ± 1.5a	62.0 ± 0.7c	64.4 ± 0.6b	59.4 ± 0.2d	5.0 ± 0.6	276 ± 36	141 ± 39
10,700	0–69	0–66	0–64	98.1 ± 1.5a	82.4 ± 0.7c	84.9 ± 0.6b	79.7 ± 0.3d	5.1 ± 0.7	286 ± 39	147 ± 43
15,700	0–98	0–95	0–93	130.4 ± 1.5a	113.7 ± 0.7c	116.4 ± 0.7b	110.1 ± 0.3d	6.3 ± 0.7	350 ± 41	202 ± 45
18,700	0–118	0–115	0–112	150.3 ± 1.5a	133.1 ± 0.8c	135.9 ± 0.7b	129.3 ± 0.4d	6.5 ± 0.8	363 ± 43	210 ± 46
21,900	0–137	0–134	0–131	170.9 ± 1.5a	152.8 ± 0.8c	155.7 ± 0.7b	149.5 ± 0.4c	6.2 ± 0.8	345 ± 44	185 ± 48
25,100	0–157	0–154	0–150	191.0 ± 1.6a	172.4 ± 0.8c	175.4 ± 0.7b	169.9 ± 0.4c	5.5 ± 0.8	306 ± 45	140 ± 49
28,300	0–176	0–173	0–170	209.5 ± 1.6a	190.5 ± 0.8c	193.5 ± 0.7b	189.3 ± 0.4c	4.3 ± 0.8	238 ± 47	69 ± 51
31,500	0–196	0–193	0–189	226.1 ± 1.6a	206.0 ± 0.84c	209.2 ± 0.7b	205.9 ± 0.4c	3.3 ± 0.9	183 ± 48	5 ± 53

constituted an aliquot of the entire 0–20 μm fraction. After a settling time of 8 h approximately, a second aliquot of 50 mL was removed by siphoning the upper 10 cm of the suspension left after the first sampling. This represented an aliquot of the 0–2 μm fraction. A third aliquot was also collected in the upper 10 cm, and centrifuged two times 35 min, at 4000 rpm. This aliquot was then filtered at 2 μm to get the hydrosoluble fraction. Fractions were then dried at 40 °C, finely ground, decarbonated and analyzed with a CHN elemental analyzer. A binocular microscope was used to check if separation of coarse mineral fractions and of light organic coarse fractions (200–2000 and 50–200 μm) was well done. No pyrogenic particles were observed. Organic carbon contents of coarse mineral fractions were then assumed to be 0 mg C g^{-1}. A sub-sample of each of the 64 selected samples was used to perform a classical textural analysis after destruction of organic matter. These texture analyses were used to evaluate the quality of the dispersion for soil particle size fractionation.

2.9. Calculation of SOC saturation

The theoretical value of SOC saturation was calculated according to the equation proposed by (Hassink, 1997):

$$SOC_{sat-pot} = 4.09 + 0.37 \times \text{particles} < 20\ \mu m \quad (4)$$

where $SOC_{sat\text{-}pot}$ is the potential SOC saturation (mg C g^{-1}) and where particles <20 μm represent the proportion of fine soil particles <20 μm (%).

To calculate the SOC saturation deficit (Angers et al., 2011; Wiesmeier et al., 2014), the estimated current SOC concentrations of the fine fraction were subtracted from the potential SOC saturation:

$$SOC_{sat-def} = SOC_{sat-pot} - SOC_{cur} \quad (5)$$

where $SOC_{sat\text{-}def}$ is the SOC saturation deficit (mg C g^{-1}) and SOC_{cur} is the current mean SOC concentration of the fine fraction <20 μm (mg C g^{-1}). The total amount of the SOC storage potential ($SOC_{stor\text{-}pot}$, Mg C ha^{-1}) was calculated multiplying $SOC_{sat\text{-}def}$ by soil bulk density and soil layer thickness.

These calculations were performed for the four depths where particle-size fractionation was done (0–10, 10–30, 70–100 and 160–180 cm). But as the equation proposed by (Hassink, 1997) was calibrated for topsoil layers, calculations for deep soil layers are only indicative.

2.10. Statistical analyses

The observed variability in a soil property Z such as SOC concentration results from complex processes operating over various spatial scales. A simple but useful statistical model for Z at a set of observations that could be spatially located, $\boldsymbol{s}_i = \{\boldsymbol{s}_1, \boldsymbol{s}_2, \cdots, \boldsymbol{s}_q\}$ is

$$Z(\boldsymbol{s}_i) = \mu(\boldsymbol{s}_i) + \varepsilon(\boldsymbol{s}_i) \quad (6)$$

where $\mu(\boldsymbol{s}_i)$ is a deterministic component and $\varepsilon(\boldsymbol{s}_i)$ is a correlated random component that can include a pure noise random one. A soil property can be correlated with other environmental variables such as, in this work, the distance to the closest tree. This can be represented in Eq. (6) by assuming that $\mu(\boldsymbol{s}_i)$ comprises an additive combination of one or more fixed effect:

$$\mu(\boldsymbol{s}_i) = \beta_0 + \sum_{j=1}^{q} \beta_j x_j(\boldsymbol{s}_i) \quad (7)$$

where $x_j (j = 1, 2, \cdots, q)$ are q auxiliary variables and $\beta_0, \ldots, \beta_q$ are the associated fixed effects. This model is referred as a Mixed Effects Model which offers a flexible framework by which to model the sources of variation and correlation that arise from grouped data (Lark et al., 2006; Pinheiro and Bates, 2000). In this work, we fitted two different linear mixed models (LMM).

We first fitted a LMM using the whole set of the bulk densities, SOC concentrations, and SOC stocks observations at the different depths. We used the *nlme* package (Pinheiro et al., 2013). Soil core ID was considered as a random effect to take into account a sample effect. These soil properties were then compared by depth and per location (control, tree row, inter-row). An ANOVA was performed on these models. We then used the *multcomp* package (Hothorn et al., 2008) to perform a post hoc analysis and determine which means differed significantly between the control, tree rows and inter-rows, using the Tukey–Kramer test, designed for unbalanced data. To study spatial influence on SOC stocks, "distance to the closest tree" was added to the LMM model, and an ANOVA was performed.

Secondly, we fitted a LMM in a geostatistical framework using the cumulated SOC stock observations for 3 depths (0–30 cm, 0–100 cm and 0–200 cm). In a spatial context, the random effects of the LMM describe spatially-correlated random variation. The LMM model is then parameterized by a global vector, called Θ, of model parameters which include the parameters of the covariance function and the fixed effects coefficients. These can be fitted to the data by a likelihood method. Lark et al. (2006) described how the maximum likelihood estimator is biased in the presence of fixed effects and suggested that the restricted maximum likelihood estimator (REML) should be applied. Following Villanneau et al. (2011) we have tested the assumption that the random effects are spatially correlated by comparing the quality of the model-fit for spatially correlated and spatially independent models (usually called pure nugget model). Webster and McBratney (1989) suggested that the Akaike information criterion (AIC, Akaike, 1974) should be used to compare different spatially correlated models. Once the parameters of

the LMM have been fitted, they may be plugged into the best linear unbiased predictor to form the empirical best linear unbiased predictor (E-BLUP) of the property at unsampled sites (Lark et al., 2006). The error variance of the E-BLUP can also be computed at any unsampled site. For this, the value of fixed effects covariates must be known at each prediction site. We therefore calculated several grids of the fixed effects with a 25 cm cell size. The use of any model of spatial variation implies that assumptions have been made about the type of variation the data exhibit. Once the model has been fitted, cross-validation can be used to confirm that these assumptions are reasonable and that the spatial model appropriately describes the variation. We therefore computed a 'leave-one-out cross-validation'. For each sampling location, $\boldsymbol{s}_i (i = 1, 2, \cdots, q)$, the value of the property at s_i was predicted by the E-BLUP upon the vector of observations excluding $Z(\boldsymbol{s}_i)$, in order to compute the standardized squared prediction error (SSPE: the squared difference between the E-BLUP and the observed value divided by the computed prediction error variance (PEV)). Under an assumption of normal prediction errors, the expected mean SSPE is 1.0 if the PEVs are reliable (which requires an appropriate variogram model), and the expected median SSPE is 0.455. The spatial analysis package *GeoR* (Ribeiro and Diggle, 2001) was used for REML fitting and kriging.

Finally, a Kruskal–Wallis test (Kruskal and Wallis, 1952) was performed to analyze SOC concentration in soil fractions per depth and per location (5 or 6 replicates). This test was followed by a post hoc analysis using Dunn's test (Dunn, 1964) with a Bonferroni correction (P-value = 0.017).

All the statistical analyses were performed using R software version 3.1.1 (R Development Core Team, 2013), at a significance level of <0.05.

3. Results

3.1. Changes in soil texture with depth

Clay, silt and sand profiles were very similar at both plots (Fig. 3). Soil texture was homogeneous in the first 50 cm. Clay and silt contents linearly increased till 100 cm soil depth to reach about 325 g kg^{-1} and 575 g kg^{-1} respectively, while sand content decreased. Soil texture did not change between 100 and 200 cm soil depth. Below 140 cm depth, clay and sand content were significantly different ($F = 71.31$, $P < 0.001$) in both plots, but the maximum difference was less than 20 g kg^{-1}.

3.2. Soil bulk densities

Soil bulk densities were significantly higher in the control plot than in the tree row at all depths except for 30–50 and 140–160 cm, and higher than in the inter-row, except for 10–30 and below 140 cm depth (Table 3). In the agroforestry system, soil bulk densities were higher in the inter-row than in the tree row for 0–10 and 10–30 cm.

3.3. Soil organic carbon concentrations

An ANOVA performed on the LMM model revealed that soil depth (F-value = 270, $P < 0.0001$) and location, i.e., tree row vs. inter-row (F-value = 171, $P < 0.0001$), were the only variables affecting significantly SOC concentrations. Distance to the closest tree had no significant effect (F-value = 1.3, $P = 0.28$). As shown in Fig. 4, for 0–10 cm, SOC concentration doubled in the tree row (21.6 ± 0.8 mg C g^{-1}) compared to the inter-row (9.8 ± 0.1 mg C g^{-1}) and to the control (9.3 ± 0.1 mg C g^{-1}), whereas the latter two were not significantly different. SOC concentration was significantly higher in the tree row than in the control plot to 120 cm soil depth, except in the 50–70 cm soil layer where no difference was observed. SOC concentration was significantly higher in the tree row than in the inter-row to 30 cm soil depth.

3.4. Soil organic carbon stocks

Fig. 5 represents SOC stocks in the agroforestry plot as a function of soil depth, location and distance to the closest tree. For a given depth and distance to the closest tree, variability of SOC stocks was high, and there was no effect of the distance to the closest tree on SOC stocks (Fig. 5). An ANOVA performed on the LMM model confirmed that SOC stocks were significantly influenced by soil depth (F-value = 483, $P < 0.0001$) and location, i.e., tree row vs. inter-row (F-value = 66, $P < 0.0001$), but not by the distance to the closest tree (F-value = 1.5, $P = 0.22$).

For an equivalent soil mass (ESM) of 4000 Mg ha^{-1} (to 26–29 cm depth), SOC stocks were significantly higher in the tree row than in the inter row and in the control (Table 2). For an ESM of 31,500 Mg ha^{-1} (to 189–196 cm depth), SOC stocks were about 20 Mg C ha^{-1} higher in the tree rows compared to the inter-rows or to the control. Cumulated SOC stocks were significantly higher in the inter-row than in the control plot to an ESM of 18,700 Mg ha^{-1} (to 112–115 cm depth), except for an ESM of 1000 Mg ha^{-1} where no difference was found (Table 2).

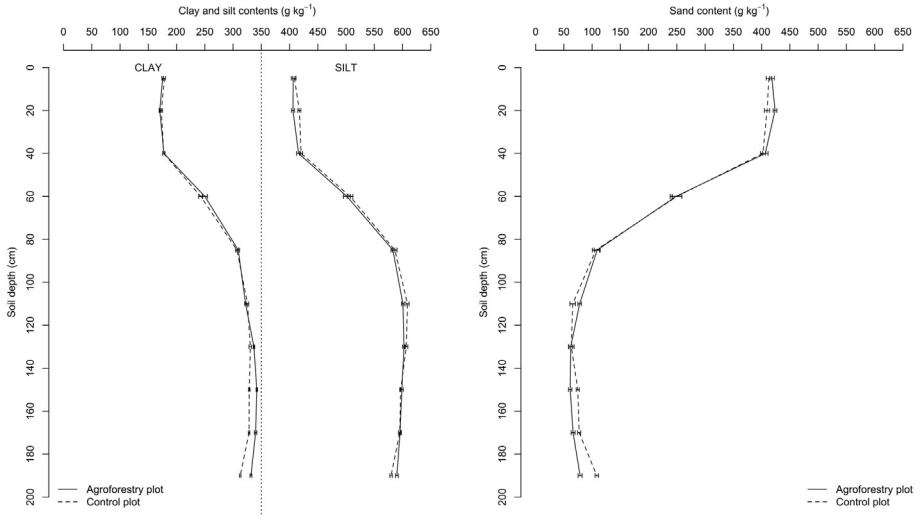

Fig. 3. Changes in soil texture with depth in the control plot and in the agroforestry plot. Error bars represent standard errors (n = 100 in the agroforestry, n = 93 in the control).

Table 3
Mean soil bulk densities (g cm^{-3}). For a given depth, means followed by the same letters do not differ significantly at $P = 0.05$. Associated errors are standard errors (40 replicates for the tree-row, 60 replicates for the inter-row, and 93 replicates for the control plot).

Depth (cm)	Agroforestry — tree row	Agroforestry — inter-row	Control plot
0–10	1.10 ± 0.02c	1.23 ± 0.03b	1.41 ± 0.01a
10–30	1.49 ± 0.01b	1.60 ± 0.02a	1.61 ± 0.00a
30–50	1.71 ± 0.01ab	1.67 ± 0.02b	1.73 ± 0.00a
50–70	1.73 ± 0.01c	1.77 ± 0.01b	1.80 ± 0.00a
70–100	1.68 ± 0.00c	1.71 ± 0.00b	1.74 ± 0.00a
100–120	1.55 ± 0.01b	1.55 ± 0.01b	1.61 ± 0.00a
120–140	1.63 ± 0.00b	1.64 ± 0.01b	1.65 ± 0.00a
140–160	1.64 ± 0.00a	1.64 ± 0.01a	1.65 ± 0.00a
160–180	1.62 ± 0.01b	1.65 ± 0.01a	1.65 ± 0.00a
180–200	1.64 ± 0.00b	1.65 ± 0.00a	1.65 ± 0.00a

At the plot scale, cumulated SOC stocks in the agroforestry plot were significantly higher than in the control plot at all depths (Table 2). For an ESM of 4000 Mg ha^{-1} (to 26–29 cm depth), SOC stocks were 40.3 ± 0.5 Mg C ha^{-1} and 35.8 ± 0.2 Mg C ha^{-1} in the agroforestry and in the control, respectively. For a soil mass of 15700 Mg ha^{-1} (to 93–98 cm depth), Δ SOC stock between the agroforestry and the control was 6.3 ± 0.7 Mg C ha^{-1}. This difference was much lower without the ESM correction (Table S1).

3.5. Soil organic carbon accumulation rates

Compared to the control, inter-rows accumulated 115 ± 33 kg C ha^{-1} yr^{-1} for an ESM of 4000 Mg ha^{-1} (26–29 cm) (Table 2), and 202 ± 45 kg C ha^{-1} yr^{-1} for an ESM of 15700 Mg ha^{-1} (93–98 cm). SOC accumulation rates in the agroforestry plot compared to the control were 248 ± 31 kg C ha^{-1} yr^{-1} for an ESM of 4000 Mg ha^{-1}, 350 ± 41 kg C ha^{-1} yr^{-1} an ESM of 15,700 Mg ha^{-1}, and 183 ± 48 kg C ha^{-1} yr^{-1} an ESM of 31,500 Mg ha^{-1} (Table 2). The SOC accumulation rates for 0–10 cm and 10–30 cm were respectively explained at 80% and 60% by the tree rows.

3.6. Spatial distribution of SOC stocks

The AIC (Table 4) of the spatially correlated model were less than that of the spatially uncorrelated model for 2 depths (0–100 cm and 0–200 cm for the agroforestry and the control plots), indicating that spatial correlation should be included in the model of variation. We tested several models of spatial variation and retained the spherical model (Webster and Oliver, 2007). For top soil depth of the two plots (0–30 cm), the AIC of the spatially uncorrelated model was slightly the smallest indicating that the residual variation could be independent once fixed effects had been included in the model. But the difference was very small so we considered the spatially correlated model for the rest of the study. The cross-validation results confirmed the validity of the fitted LMM. The nugget to sill ratio measures the unexplained part of the observed variability. The smallest value was observed for the 0–200 cm depth in the control plot and the higher was observed for the 0–30 cm depth in both plots. When mapping the SOC stocks for three fixed depths with the BLUP in the two plots, a clear pattern can be observed in the agroforestry plot, with high SOC stocks in the tree rows (Fig. 6). The fitted fixed effects indicate that, in average, the SOC stocks were 15 to 20 Mg C ha^{-1} higher in the tree rows to 30 to 200 cm depth (Table 4). At the opposite, the control plot did not exhibit any spatial pattern.

3.7. Organic carbon distribution in soil fractions

An average mass yield of 98% and an average carbon yield of 96% were obtained, showing the quality of the particle size fractionation. Furthermore, the variation between soil texture and soil fractionation was only 5–6% (data not shown). Soil segments used for soil fractionation had similar total SOC concentrations compared to mean SOC

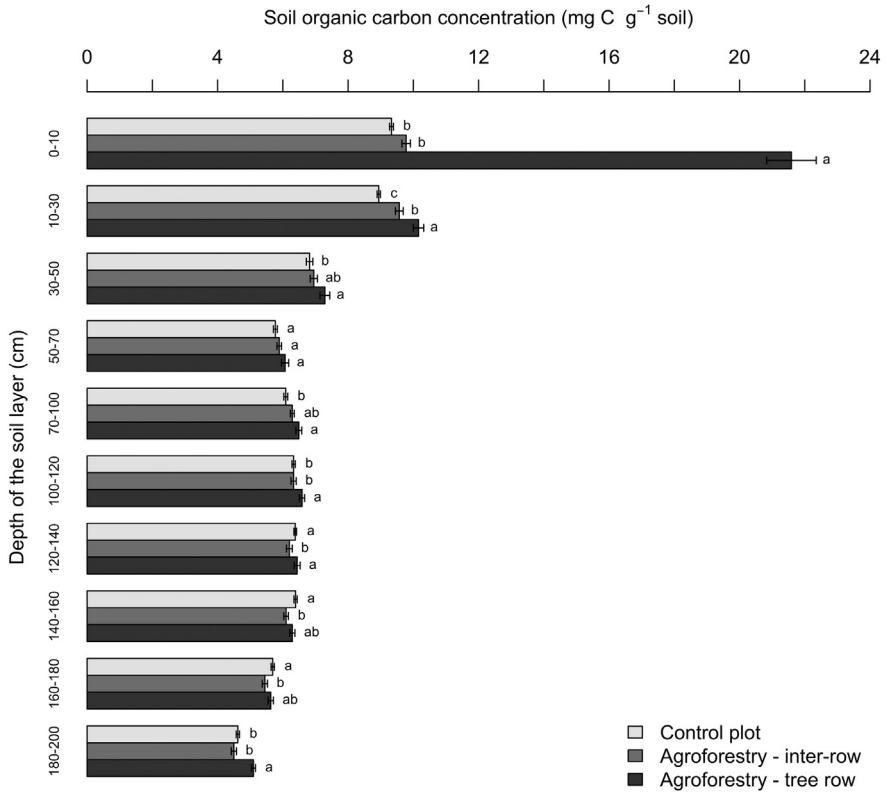

Fig. 4. Soil organic carbon concentration (mg C g^{-1} soil) of soil layers to 2-m depth in the control plot and in the agroforestry plot. Error bars represent standard errors (n = 40 for the tree row, n = 60 for the inter-row, and n = 93 for the control). Significantly (P-value < 0.05) different SOC concentrations per depth are followed by different letters.

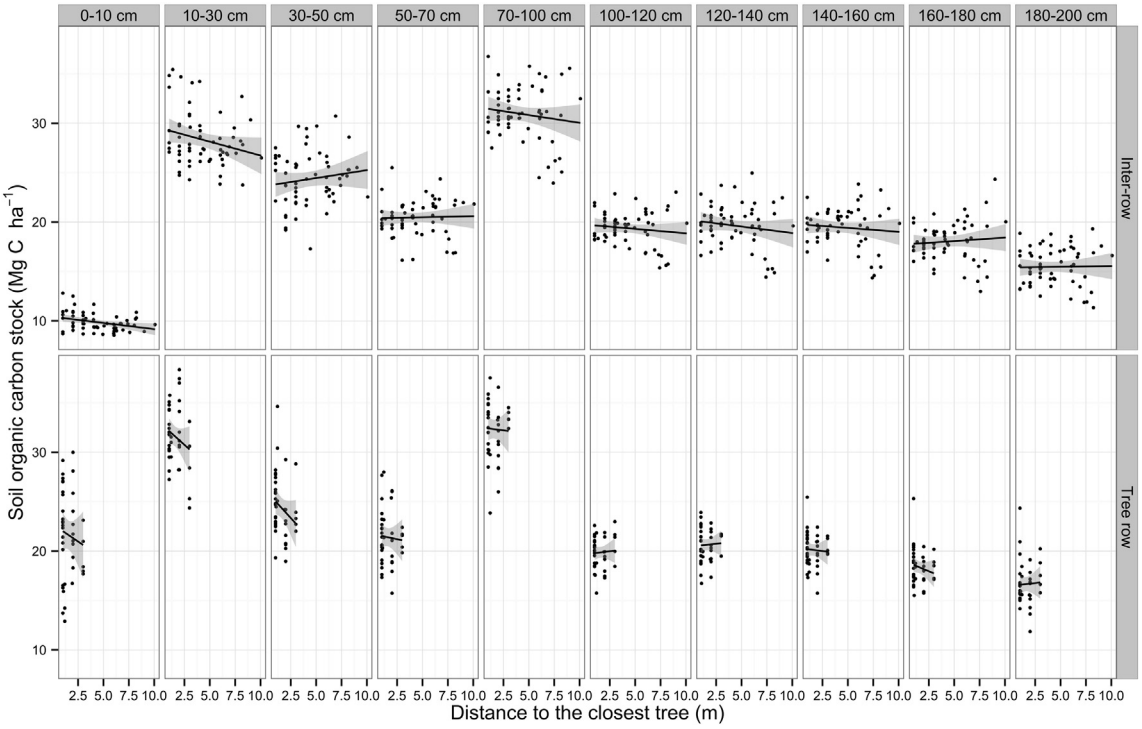

Fig. 5. Soil organic carbon stocks (Mg C ha^{-1}) in the agroforestry plot as a function of depth, location (tree row vs. inter-row) and distance to the closest tree. The lines represent the regression lines fitted using soil samples per investigated depth. The gray shades display the prediction confidence interval at the 0.95 level.

concentrations at the same depth (Fig. S2). However, the small differences found between SOC concentrations in the inter row and in the control was not visible with the soil segments used for fractionation.

For 0–10 cm depth, the distribution of OC in particle size fractions was strongly modified in the tree rows, with an important increase of C in particulate organic matter (POM) fractions (50–200 μm and 200–2000 μm) compared to the inter-row and to the control (Fig. 7). An increase of C in silt size fractions (2–20 μm and 20–50 μm) of the tree rows compared to the inter row and to the control was also observed. Significantly higher C concentrations in the clay fraction (0–2 μm) were observed in the tree row than in the inter-row (Fig. S3), but it was not the case for the amount of C in the clay fraction per gram of soil (Fig. 7).

Similar trends in C distribution in fractions were observed at 10–30 cm depth compared to 0–10 cm, although with much smaller differences (Figs. 7, S3). At deeper depths (70–100 and 160–180 cm) there were no differences between the three locations (tree row, inter-row and control) except a lower amount of C in the soluble fraction in the tree row. The potential SOC saturation of particles <20 μm was not reached at any depths (Table 5), and the SOC deficit was high. The saturation capacity was far from being reached, as it amounted 17 to 40% of saturation capacity in the tree rows.

3.8. Distribution of additional OC in soil fractions

For 0–10 cm depth, the additional OC stored between the tree row and the inter-row was explained at 80% by POM fractions, at 15% by silt size fractions, and at 5% by clay fraction, whereas the additional OC stored between the tree row and the control was explained at 80% by POM and at 20% by silt size fractions (Fig. 7). For 10–30 cm, the additional SOC storage between the tree row and the inter-row was explained at 50% by POM fractions, at 25% by coarse and fine silt fractions, and at 25% by clay fraction (Fig. 7), whereas when comparing the tree row and the control these numbers were of 50% (POM) and 50% (silt).

4. Discussion

4.1. A shallow additional SOC storage

Sampling to 2-m soil depth indicated that the 0–30 cm soil layer contained less than 20% of total SOC stocks to 2-m depth, demonstrating the importance of deeper soil layers for storing SOC (Harper and Tibbett, 2013; Jobbagy and Jackson, 2000). SOC stocks observed in 0–30 cm, from 36 to 41 Mg C ha^{-1}, were comparable to reported values for the Mediterranean region, i.e., 25 to 50 Mg C ha^{-1} (Martin et al., 2011;

Table 4
Summary of selected models fitted to the data on cumulated soil organic carbon stocks at 3 depths (0–30 cm, 0–100 cm and 0–200 cm) for the 2 plots, and cross validation. SSPE, standardized squared prediction errors; ME, mean error (Mg C ha^{-1}); RMSQE, root mean squared error (Mg C ha^{-1}); AIC, AIC of the spatially correlated model; AIC.ns, AIC of the non-spatially correlated model; β_0 and β_1 the fixed effects (Mg C ha^{-1}). Bold characters represent the smallest AIC for each depth. The medians and the mean of the cross validation statistics are within the 95% confidence interval.

	Depth (cm)	Mean SSPE	Median SSPE	ME	RMQSE	AIC	AIC.ns	β_0	β_1	Nugget	Sill	Range	Nugget to sill ratio
Agroforestry	0–30	0.99	0.36	−0.004	20.7	585	**583**	38.1	14.8	19.7	1.3	15.2	0.94
	0–100	0.99	0.45	−0.010	43.3	**662**	665	114.1	16.4	36.0	16.3	12.8	0.69
	0–200	0.98	0.39	0.055	123.1	**769**	780	207.1	19.4	97.8	79.2	12.9	0.55
Control	0–30	1.01	0.33	0.000	2.6	361	**357**	35.9	–	2.4	0.2	19.4	0.93
	0–100	1.01	0.50	0.061	25.7	**578**	579	111.2	–	20.2	11.0	12.6	0.65
	0–200	0.98	0.40	0.519	57.5	**665**	681	208.9	–	16.4	85.8	6.3	0.16

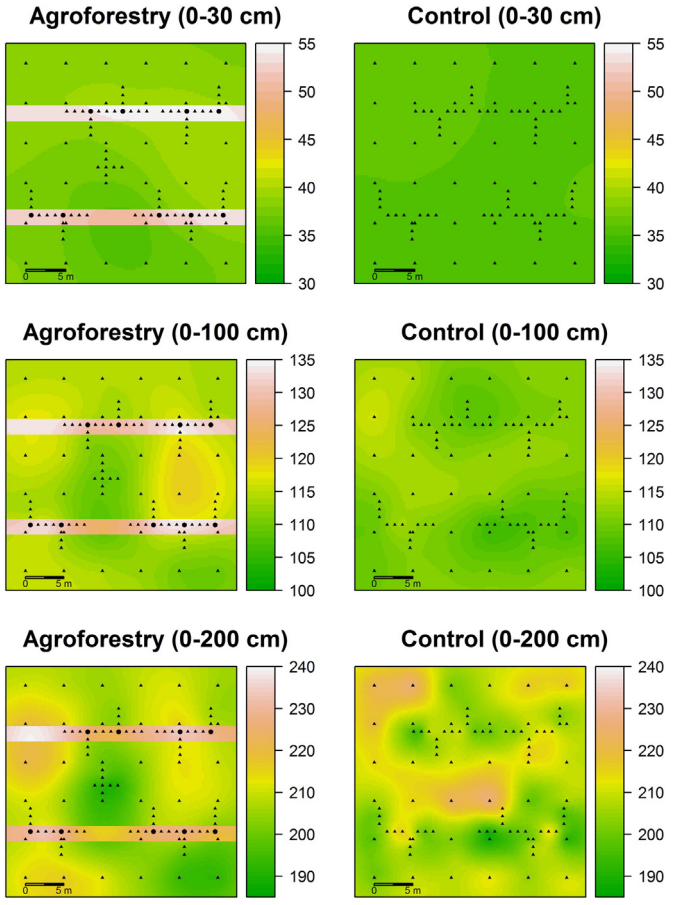

Fig. 6. Krieged maps of cumulated soil organic carbon stocks (Mg C ha^{-1}) in the agroforestry and in the control plot.

Muñoz-Rojas et al., 2012). Additional SOC storage in the agroforestry system compared to the agricultural system was mainly observed up to 30 cm soil depth in the inter-row and up to 50 cm in the tree row.

A companion study at the same site indicated that 60% of additional OM inputs (leaf litter, aboveground and belowground biomass of the natural vegetation in the tree row, tree fine roots) to 2 m depth in the agroforestry plot compared to the control plot were located in the first 50 cm (unpublished data). Even if 50% of tree fine root density was found between 1 and 4 m soil depth (Cardinael et al., 2015), it was also proven at this site (Germon et al., submitted for publication) and at other sites (Hendrick and Pregitzer, 1996) that the turnover rate of fine roots decreased with increasing depth, resulting in low OM inputs in deep soil layers. Time since the tree planting (18 years) is probably not long enough to detect changes in SOC stocks at deeper soil depths considering low organic inputs below 1 m depth. For 2012, organic C input due to tree fine root mortality was estimated to be less than 150 kg C ha^{-1} for 100–200 cm soil depth. Below 1.2 m soil depth, delta of cumulated SOC stocks between the agroforestry and the control plot decreased, due to higher SOC concentrations and stocks in the control at these depths. These higher SOC concentrations were linked to higher SOC concentrations in the clay fraction. This difference may be due to pre-experimental soil heterogeneity, the soil in the agroforestry plot may have had a lower level of SOC below 1.2 m depth before tree planting. An initial heterogeneity was also proposed by Upson and Burgess (2013) who found higher SOC stocks at depth in a control plot compared to an agroforestry plot in an experimental site in England. This shows the limit of paired comparisons – or synchronic studies – to evaluate SOC changes after land use change (Junior et al., 2013; Olson et al., 2014), and pleads for long-term diachronic studies in agroforestry systems. An alternative explanation could be a positive priming effect, i.e., the acceleration of native SOC decomposition by the supply of fresh organic carbon (Fontaine et al., 2004, 2007) from the trees. However, this seems highly unlikely since positive priming effect could not explain such a high C loss of about 3.2 Mg C ha^{-1} between 1.2 and 2.0 m soil depth in 18 years, i.e., about 180 kg C ha^{-1} yr^{-1}. Another hypothesis to explain higher SOC stocks below 1.2 m depth in the control plot is a different belowground water regime between the two plots. Water table depth at this site is known to be very variable (between 5 and 7 m). A shallower water table in the agroforestry plot compared to the control plot may promote capillary action, and therefore cause wetting–drying cycles that could enhance SOM decomposition in deep soil layers (Borken and Matzner, 2009).

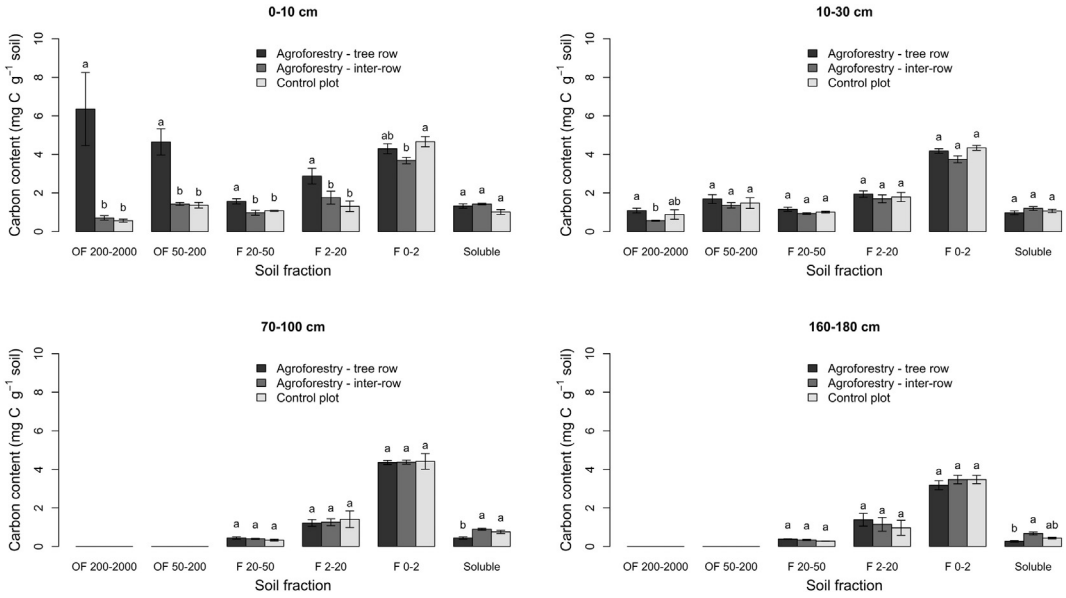

Fig. 7. Organic carbon contents in each soil fraction (mg C g^{-1} soil). Error bars represent standard errors (n = 6 in the control, n = 5 in the inter-row and in the tree row). OF = Organic fraction, F = organo-mineral fraction. 0–2, 2–20, 20–50, 50–200 and 200–2000 represent particle size (μm). Means followed by the same letters do not differ significantly at $P = 0.017$ (Dunn's test with Bonferroni correction).

Table 5
Soil organic carbon saturation of the fractionated soil samples in the agroforestry plot. $SOC_{sat-pot}$, potential SOC saturation (mg C g^{-1}); SOC_{cur}, current mean SOC concentration of the fine fraction <20 μm (mg C g^{-1}); $SOC_{sat-def}$, SOC saturation deficit (mg C g^{-1}); $SOC_{stor-pot}$, total amount of the SOC storage potential (Mg C ha^{-1}). Associated errors are standard errors (n = 5). Values of SOC saturation for deep soil layers are only indicative.

Depth (cm)	$SOC_{sat-pot}$ (mg C g^{-1})	SOC_{cur} (mg C g^{-1})		$SOC_{sat-def}$ (mg C g^{-1})		$\frac{SOC_{cur}}{SOC_{sat-pot}}$		$SOC_{stor-pot}$ (Mg C ha^{-1})
	Agroforestry	Tree row	Inter-row	Tree row	Inter-row	Tree row	Inter-row	Agroforestry
0–10	18.0 ± 0.4	7.2 ± 0.3	5.4 ± 0.3	10.3 ± 0.4	13.1 ± 0.4	40%	30%	15.3 ± 0.4
10–30	18.7 ± 0.4	6.1 ± 0.1	5.4 ± 0.1	12.6 ± 0.3	13.3 ± 0.3	33%	29%	41.8 ± 0.9
70–100	32.9 ± 0.8	5.6 ± 0.1	5.6 ± 0.1	26.9 ± 0.7	27.6 ± 0.4	17%	17%	140.7 ± 1.9
160–180	32.0 ± 1.1	4.6 ± 0.2	4.6 ± 0.3	26.8 ± 0.7	28.1 ± 0.9	14%	14%	91.9 ± 2.4

4.2. Tree rows and SOC storage in agroforestry systems

The high SOC stocks observed in tree rows accounted for an important part of SOC stocks of the agroforestry plot even though tree rows only represented 16% of the surface area. In a poplar (*Populus* L.) silvoarable agroforestry experiment in England, Upson and Burgess (2013) also found that the SOC concentration was greater in the top 40 cm under the tree row (19.6 mg C g^{-1}) in the agroforestry treatment than in the cropped alleys (17 mg C g^{-1}), or the arable control (17.1 mg C g^{-1}). Tree rows are comparable to a natural permanent pasture with trees, given that spontaneous herbaceous vegetation grows and that the soil is not tilled. Conversion of arable lands to permanent grasslands is recognized as an efficient land use for climate change mitigation (Soussana et al., 2004). Grasslands can accumulate SOC at a very high rate. For instance, it was estimated on about 20 years old field experiments that conversion from crop cultivation to pasture stored SOC at a rate of 1.01 Mg C ha^{-1} yr^{-1} in 0–30 cm (Conant et al., 2001). In our case, SOC accumulation rate in the tree rows was 0.94 ± 0.09 Mg C ha^{-1} yr^{-1} in 0–30 cm. Management of tree rows could therefore have an important role in improving agroforestry systems in terms of SOC storage. Improved grass species could be sown in the tree rows, as well as shrubs between trees. Further research should focus on this aspect to evaluate benefits in terms of SOC storage and biodiversity for instance.

4.3. Homogeneous distribution of SOC stocks in the cropped alley

There was no significant effect of the distance to the trees on SOC stocks at all depths, either in the tree row or in the inter-row. This was also indicated by the maps of the SOC stocks. Tree density was high at this site, and walnuts were about 13 m in height, which is also the distance between two tree rows. This could explain the homogeneous distribution of leaf litterfall observed in the plot (personal observation). In a similar agroforestry system in terms of tree density in Canada, Bambrick et al. (2010) and Peichl et al. (2006) also found no effect of the distance to the trees on SOC stocks to 20 cm depth. They also suggested that the 18 m high poplar trees distributed litterfall equally in the cropped alleys. Close to the tree rows (1 to 2 m distance), the intercrop had a lower yield (15% less in 2012) compared to the middle of the inter-row at the study site (Dufour et al., 2013). On the contrary, tree fine root density was higher close to the tree rows (2.79 t DM ha^{-1} between 0 and 1.5 m from the tree row in the inter row, and to 4-m soil depth) than in the middle of the inter-rows (1.32 t DM ha^{-1} between 3 and 4.5 m from the tree row in the inter row, and to 4-m soil depth) (Cardinael et al., 2015). Thus, lower carbon inputs from crop residues close to the tree rows may be counterbalanced with higher inputs from tree fine root mortality, explaining homogeneous distribution of SOC stocks within the inter-row (Bambrick et al., 2010; Peichl et al., 2006). In the tree row, homogeneous distribution of SOC stocks may be explained by the short distance between trees and by the presence of abundant herbaceous vegetation.

4.4. Agroforestry systems: an efficient land use to improve SOC stocks

Compared to other agroforestry systems having about the same tree density, a lower SOC accumulation rate in 0–30 cm (0.25 Mg C ha^{-1} yr^{-1}) was observed at our site. Peichl et al. (2006) reported a SOC accumulation rate of 1.04 Mg C ha^{-1} yr^{-1} (0–20 cm) in a 13-year old temperate barley (*Hordeum vulgare* L.)-poplar intercropping system (111 trees ha^{-1}). In a 21-year old agroforestry system in Canada where poplars were intercropped with a rotation of wheat (*Triticum aestivum* L.), soybean (*Glycine max* (L.) Merr.) and corn (*Zea mays* L.), Bambrick et al. (2010) estimated a SOC accumulation rate of 0.30 Mg C ha^{-1} yr^{-1} (0–20 cm). Our lower accumulation rate may be explained by warmer climate, higher temperatures enhancing OM decomposition (Hamdi et al., 2013; Conant et al., 2011). Moreover, valuable hardwood species like walnut trees have a slower growing rate than fast growing species like poplar (Teck and Hilt, 1991), and therefore for a same tree age, the amount of OC inputs (leaflitter, fine roots) to the soil is lower for slow growing species.

Together with other climate-smart farming practices (Lipper et al., 2014), alley-cropping agroforestry systems have the potential to enhance SOC stocks and to contribute to climate change mitigation (Nair et al., 2010; Pellerin et al., 2013). No-till farming is a commonly cited agricultural practice supposed to have a positive impact on SOC stocks. But recent meta-analyses showed this practice had no effect on SOC stocks to 40 cm depth (Luo et al., 2010) or a smaller one (0.23 Mg C ha^{-1} yr^{-1} to 30 cm depth) than previously estimated (Virto et al., 2011). A meta-analysis also revealed that the inclusion of cover crops in cropping systems could accumulate SOC at a rate of 0.32 ± 0.08 Mg C ha^{-1} yr^{-1} to a depth of 22 cm (Poeplau and Don, 2015). At our site, we found a mean SOC accumulation rate of 0.12 in 0–30 cm in the inter-rows compared to the control. This rate reached 0.25 Mg C ha^{-1} yr^{-1} for the whole agroforestry system. A companion study at this site estimated that the tree aboveground C stock was 117 ± 21 kg C $tree^{-1}$ (unpublished data). With 110 trees ha^{-1}, total organic carbon (SOC to 1 m soil depth + aboveground tree C) accumulation rate was 1.11 ± 0.13 Mg C ha^{-1} yr^{-1}, making agroforestry systems a possible land use to help mitigating climate change (Lal, 2004a, 2004b; Lorenz and Lal, 2014).

4.5. A long-term SOC storage?

Most of additional SOC in the agroforestry plot compared to the control plot was located in coarse soil fractions (50–200 μm and 200–2000 μm). These soil fractions are assumed to contain labile fractions (Balesdent et al., 1998), that are not stabilized by interaction with clays and thus prone to be decomposed by soil microorganisms. Our site might not be old enough to observe a difference in the fine soil fractions as changes in the clay fractions are often long-term processes (Balesdent, 1996; Balesdent et al., 1988). For example, Takimoto et al. (2008) found in a 35-year-old *Faidherbia albida* parkland in Mali, that the silt + clay soil fraction (<53 μm) was enriched in C at depth compared with treeless systems. But on the other hand,

Howlett et al. (2011) did not observe any difference for the same soil fraction in a 80 year-old Dehesa cork oak (*Quercus suber* L.) silvopasture, but they found that C storage in the macroaggregate fraction (250–2000 mm) was 68% greater underneath versus away from the tree canopy (in 0–25 cm). Several studies have demonstrated that protection of C within the macroaggregate size class was affected by afforestation (Del Galdo et al., 2003; Denef et al., 2013) and cessation of tillage (Tan et al., 2007). The fractionation method that was used in this study disrupted macroaggregates (von Lützow et al., 2007), and part of these labile fractions could be located within them and therefore be physically protected from decomposition by soil microorganisms (Six et al., 2000; Puget et al., 2000). Further work will focus on this aspect in order to estimate the amount of particulate organic matter located in soil aggregates. Calculation of SOC saturation revealed a high deficit of SOC of this soil compared to the theoretical value, suggesting that accumulation of SOC due to the agroforestry system could continue for decades before reaching saturation.

5. Conclusion

This study showed the potential of agroforestry systems to increase SOC stocks. However, despite a deep tree rooting system, additional SOC was mainly located in topsoil layers, and in labile organic fractions, making this C storage vulnerable. Tree rows were shown to be a key factor for SOC storage in alley cropping systems. Combining agroforestry systems with no-till or permanent cover systems could be a very efficient way to increase SOC stocks, but more research is needed on this aspect. To fully estimate the impact of agroforestry systems on SOC sequestration, other aspects should be taken into account. For instance, higher SOC stocks in the inter-rows could increase soil fertility and reduce the need for chemical fertilizer, contributing indirectly to a reduction of greenhouse gases emissions; further work should therefore focus on nutrient cycling in these systems.

Supplementary data to this article can be found online at http://dx.doi.org/10.1016/j.geoderma.2015.06.015.

Acknowledgments

This study was financed by the French Environment and Energy Management Agency (ADEME), following a call for proposals as part of the REACCTIF program (Research on Climate Change Mitigation in Agriculture and Forestry). This work was part of the funded project AGRIPSOL (Agroforestry for Soil Protection, 1260C0042), coordinated by Agroof. R. Cardinael was also supported by La Fondation de France. We are very grateful to our colleagues for their help with field and laboratory work and logistics, including Daniel Billiou (UPMC), Emmanuel Bourdon (IRD), Jean-François Bourdoncle (INRA), Lydie Dufour (INRA), Claude Hammecker (IRD), Alain Sellier (INRA) and Manon Villeneuve (IRD). We are also grateful to Valérie Viaud (INRA) for her valuable comments concerning the sampling design and geostatistics, and to Michael Clairotte (INRA) for his help concerning analyses of the VNIR spectra. We also thank all students without whom this work would not have been possible, especially Catalina Gomà Pumarino, Guillermo Lobos Norambuena, and Eric Zassi.

References

Akaike, H., 1974. A new look at the statistical model identification. IEEE Trans. Autom. Control 19, 716–723.
Albrecht, A., Kandji, S.T., 2003. Carbon sequestration in tropical agroforestry systems. Agric. Ecosyst. Environ. 99, 15–27.
Angers, D.A., Arrouays, D., Saby, N.P.A., Walter, C., 2011. Estimating and mapping the carbon saturation deficit of French agricultural topsoils. Soil Use Manag. 27, 448–452.
Balesdent, J., 1996. The significance of organic separates to carbon dynamics and its modelling in some cultivated soils. Eur. J. Soil Sci. 47, 485–493.
Balesdent, J., Balabane, M., 1996. Major contribution of roots to soil carbon storage inferred from maize cultivated soils. Soil Biol. Biochem. 28, 1261–1263.
Balesdent, J., Wagner, G.H., Mariotti, A., 1988. Soil organic matter turnover in long-term field experiments as revealed by carbon-13 natural abundance. Soil Sci. Soc. Am. J. 52, 118–124.
Balesdent, J., Besnard, E., Arrouays, D., Chenu, C., 1998. The dynamics of carbon in particle-size fractions of soil in a forest-cultivation sequence. Plant Soil 201, 49–57.
Bambrick, A.D., Whalen, J.K., Bradley, R.L., Cogliastro, A., Gordon, A.M., Olivier, A., Thevathasan, N.V., 2010. Spatial heterogeneity of soil organic carbon in tree-based intercropping systems in Quebec and Ontario, Canada. Agrofor. Syst. 79, 343–353.
Bauhus, J., van der Meer, P., Kanninen, M., 2010. Ecosystem Goods and Services from Plantation Forests. Earthscan, London, UK.
Bellon-Maurel, V., Fernandez-Ahumada, E., Palagos, B., Roger, J.-M., McBratney, A., 2010. Critical review of chemometric indicators commonly used for assessing the quality of the prediction of soil attributes by NIR spectroscopy. Trends Anal. Chem. 29, 1073–1081.
Bergeron, M., Lacombe, S., Bradley, R.L., Whalen, J., Cogliastro, A., Jutras, M.-F., Arp, P., 2011. Reduced soil nutrient leaching following the establishment of tree-based intercropping systems in eastern Canada. Agrofor. Syst. 83, 321–330.
Bird, J.A., Torn, M.S., 2006. Fine roots vs. needles: a comparison of 13C and 15N dynamics in a ponderosa pine forest soil. Biogeochemistry 79, 361–382.
Borken, W., Matzner, E., 2009. Reappraisal of drying and wetting effects on C and N mineralization and fluxes in soils. Glob. Change Biol. 15, 808–824.
Brown, D.J., Shepherd, K.D., Walsh, M.G., Dewayne Mays, M., Reinsch, T.G., 2006. Global soil characterization with VNIR diffuse reflectance spectroscopy. Geoderma 132, 273–290.
Cardinael, R., Mao, Z., Prieto, I., Stokes, A., Dupraz, C., Jourdan, C., 2015. Competition with winter crops induces deeper rooting of walnut trees in a Mediterranean alley cropping agroforestry system. Plant Soil 391, 219–235.
Chang, C., Laird, D.A., Mausbach, M.J., Hurburgh, C.R., 2001. Near-infrared reflectance spectroscopy—principal components regression analyses of soil properties. Soil Sci. Soc. Am. J. 65, 480–490.
Chenu, C., Plante, A.F., 2006. Clay-sized organo–mineral complexes in a cultivation chronosequence: revisiting the concept of the "primary organo–mineral complex". Eur. J. Soil Sci. 57, 596–607.
Clough, Y., Barkmann, J., Juhrbandt, J., Kessler, M., Wanger, T.C., Anshary, A., Buchori, D., Cicuzza, D., Darras, K., Putra, D.D., Erasmi, S., Pitopang, R., Schmidt, C., Schulze, C.H., Seidel, D., Steffan-Dewenter, I., Stenchly, K., Vidal, S., Weist, M., Wielgoss, A.C., Tscharntke, T., 2011. Combining high biodiversity with high yields in tropical agroforests. PNAS 108, 8311–8316.
Conant, R.T., Paustian, K., Elliott, E.T., 2001. Grassland management and conversion into grassland: effects on soil carbon. Ecol. Appl. 11, 343–355.
Conant, R.T., Ryan, M.G., Ågren, G.I., Birge, H.E., Davidson, E.A., Eliasson, P.E., Evans, S.E., Frey, S.D., Giardina, C.P., Hopkins, F.M., Hyvönen, R., Kirschbaum, M.U.F., Lavallee, J.M., Leifeld, J., Parton, W.J., Megan Steinweg, J., Wallenstein, M.D., Martin Wetterstedt, J.Å., Bradford, M.A., 2011. Temperature and soil organic matter decomposition rates — synthesis of current knowledge and a way forward. Glob. Change Biol. 17, 3392–3404.
Del Galdo, I., Six, J., Peressotti, A., Cotrufo, M.F., 2003. Assessing the impact of land-use change on soil C sequestration in agricultural soils by means of organic matter fractionation and stable C isotopes. Glob. Change Biol. 9, 1204–1213.
Denef, K., Galdo, I. Del, Venturi, A., Cotrufo, M.F., 2013. Assessment of soil C and N stocks and fractions across 11 European soils under varying land uses. Open J. Soil Sci. 3, 297–313.
Dufour, L., Metay, A., Talbot, G., Dupraz, C., 2013. Assessing light competition for cereal production in temperate agroforestry systems using experimentation and crop modelling. J. Agron. Crop Sci. 199, 217–227.
Dunn, O.J., 1964. Multiple comparisons using rank sums. Technometrics 6, 241–252.
Ellert, B.H., Bettany, J.R., 1995. Calculation of organic matter and nutrients stored in soils under contrasting management regimes. Can. J. Soil Sci. 75, 529–538.
Ellert, B.H., Janzen, H.H., Entz, T., 2002. Assessment of a method to measure temporal change in soil carbon storage. Soil Sci. Soc. Am. J. 66, 1687–1695.
Fontaine, S., Bardoux, G., Abbadie, L., Mariotti, A., 2004. Carbon input to soil may decrease soil carbon content. Ecol. Lett. 7, 314–320.
Fontaine, S., Barot, S., Barré, P., Bdioui, N., Mary, B., Rumpel, C., 2007. Stability of organic carbon in deep soil layers controlled by fresh carbon supply. Nature 450, 277–281.
Gale, W.J., Cambardella, C.A., Bailey, T.B., 2000. Root-derived carbon and the formation and stabilization of aggregates. Soil Sci. Soc. Am. J. 64, 201.
Gavinelli, E., Feller, C., Larré-Larrouy, M., Bacye, B., Djegui, N., Nzila, J. de D., 1995. A routine method to study soil organic matter by particle-size fractionation: examples for tropical soils. Commun. Soil Sci. Plant Anal. 26, 1749–1760.
Germon, A., Cardinael, R., Prieto, I., Mao, Z., Kim, J.H., Stokes, A., Dupraz, C., Laclau, J.-P., Jourdan, C., 2015. Unexpected phenology and lifespan of shallow and deep fine roots of walnut trees grown in a Mediterranean agroforestry system (submitted for publication).
Gras, J.-P., Barthès, B.G., Mahaut, B., Trupin, S., 2014. Best practices for obtaining and processing field visible and near infrared (VNIR) spectra of topsoils. Geoderma 214–215, 126–134.
Haile, S.G., Nair, V.D., Nair, P.K.R., 2010. Contribution of trees to carbon storage in soils of silvopastoral systems in Florida, USA. Glob. Change Biol. 16, 427–438.
Hamdi, S., Moyano, F., Sall, S., Bernoux, M., Chevallier, T., 2013. Synthesis analysis of the temperature sensitivity of soil respiration from laboratory studies in relation to incubation methods and soil conditions. Soil Biol. Biochem. 58, 115–126.
Harper, R.J., Tibbett, M., 2013. The hidden organic carbon in deep mineral soils. Plant Soil 368, 641–648.
Harris, D., Horwath, W.R., Van Kessel, C., 2001. Acid fumigation of soils to remove carbonates prior to total organic carbon or carbon-13 isotopic analysis. Soil Sci. Soc. Am. J. 65, 1853–1856.

Hassink, J., 1997. The capacity of soils to preserve organic C and N by their association with clay and silt particles. Plant Soil 191, 77–87.
Hendrick, R.L., Pregitzer, K.S., 1996. Temporal and depth-related patterns of fine root dynamics in northern hardwood forests. J. Ecol. 84, 167–176.
Hothorn, T., Bretz, F., Westfall, P., 2008. Simultaneous inference in general parametric models. Biom. J. 50, 346–363.
Howlett, D.S., Moreno, G., Mosquera Losada, M.R., Nair, P.K.R., Nair, V.D., 2011. Soil carbon storage as influenced by tree cover in the Dehesa cork oak silvopasture of central-western Spain. J. Environ. Monit. 13, 1897–1904.
IUSS Working Group WRB, 2007. World Reference Base for Soil Resources 2006, first update 2007. World Soil Resources Reports No. 103. FAO, Rome.
Jobbagy, E.G., Jackson, R.B., 2000. The vertical distribution of soil organic carbon and its relation to climate and vegetation. Ecol. Appl. 10, 423–436.
Jordan, C.F., 2004. Organic farming and agroforestry: alley cropping for mulch production for organic farms of southeastern United States. Agrofor. Syst. 61–62, 79–90.
Junior, C.C., Corbeels, M., Bernoux, M., Piccolo, M.C., Neto, M.S., Feigl, B.J., Cerri, C.E.P., Cerri, C.C., Scopel, E., Lal, R., 2013. Assessing soil carbon storage rates under no-tillage: comparing the synchronic and diachronic approaches. Soil Tillage Res. 134, 207–212.
Kennard, R.W., Stone, L.A., 1969. Computer aided design of experiments. Technometrics 11, 137–148.
Kruskal, W.H., Wallis, W.A., 1952. Use of ranks in one-criterion variance analysis. J. Am. Stat. Assoc. 47, 583–621.
Lal, R., 2004a. Soil carbon sequestration impacts on global climate change and food security. Science 304 (80-), 1623–1627.
Lal, R., 2004b. Soil carbon sequestration to mitigate climate change. Geoderma 123, 1–22.
Lark, R.M., Cullis, B.R., Welham, S.J., 2006. On spatial prediction of soil properties in the presence of a spatial trend: the empirical best linear unbiased predictor (E-BLUP) with REML. Eur. J. Soil Sci. 57, 787–799.
Lipper, L., Thornton, P., Campbell, B.M., Baedeker, T., Braimoh, A., Bwalya, M., Caron, P., Cattaneo, A., Garrity, D., Henry, K., Hottle, R., Jackson, L., Jarvis, A., Kossam, F., Mann, W., McCarthy, N., Meybeck, A., Neufeldt, H., Remington, T., Sen, P.T., Sessa, R., Shula, R., Tibu, A., Torquebiau, E.F., 2014. Climate-smart agriculture for food security. Nat. Clim. Change 4, 1068–1071.
Lorenz, K., Lal, R., 2014. Soil organic carbon sequestration in agroforestry systems. A review. Agron. Sustain. Dev. 34, 443–454.
Luo, Z., Wang, E., Sun, O.J., 2010. Can no-tillage stimulate carbon sequestration in agricultural soils? A meta-analysis of paired experiments. Agric. Ecosyst. Environ. 139, 224–231.
Martens, H., Naes, T., 1989. Multivariate Calibration. John Wiley & Sons, Ltd., Chichester.
Martin, M.P., Wattenbach, M., Smith, P., Meersmans, J., Jolivet, C., Boulonne, L., Arrouays, D., 2011. Spatial distribution of soil organic carbon stocks in France. Biogeosciences 8, 1053–1065.
Millennium Ecosystem Assessment, 2005. Ecosystems and Human Well-being: Synthesis. Island Press, Washington, DC.
Mulia, R., Dupraz, C., 2006. Unusual fine root distributions of two deciduous tree species in southern France: what consequences for modelling of tree root dynamics? Plant Soil 281, 71–85.
Muñoz-Rojas, M., Jordán, A., Zavala, L.M., De la Rosa, D., Abd-Elmabod, S.K., Anaya-Romero, M., 2012. Organic carbon stocks in Mediterranean soil types under different land uses (Southern Spain). Solid Earth 3, 375–386.
Nair, P.K.R., 2012. Carbon sequestration studies in agroforestry systems: a reality-check. Agrofor. Syst. 86, 243–253.
Nair, P.K.R., Nair, V.D., Kumar, B.M., Showalter, J.M., 2010. Carbon sequestration in agroforestry systems. Advances in Agronomy, pp. 237–307.
Oades, J., 1995. An overview of processes affecting the cycling of organic carbon in soils. In: Zepp, R.G., Sonntag, C. (Eds.), Role of Non-Living Organic Matter in the Earth's Carbon Cycle. John Wiley, pp. 293–303.
Oelbermann, M., Voroney, R.P., 2007. Carbon and nitrogen in a temperate agroforestry system: using stable isotopes as a tool to understand soil dynamics. Ecol. Eng. 29, 342–349.
Oelbermann, M., Voroney, R.P., Gordon, A.M., 2004. Carbon sequestration in tropical and temperate agroforestry systems: a review with examples from Costa Rica and southern Canada. Agric. Ecosyst. Environ. 104, 359–377.
Olson, K.R., Al-Kaisi, M., Lal, R., Lowery, B., 2014. Examining the paired comparison method approach for determining soil organic carbon sequestration rates. J. Soil Water Conserv. 69, 193A–197A.
Pandey, D.N., 2002. Carbon sequestration in agroforestry systems. Clim. Policy 2, 367–377.
Peichl, M., Thevathasan, N.V., Gordon, A.M., Huss, J., Abohassan, R.A., 2006. Carbon sequestration potentials in temperate tree-based intercropping systems, southern Ontario, Canada. Agrofor. Syst. 66, 243–257.
Pellerin, S., Bamière, L., Angers, D., Béline, F., Benoît, M., Butault, J.P., Chenu, C., Colnenne-David, C., De Cara, S., Delame, N., Doreau, M., Dupraz, P., Faverdin, P., Garcia-Launay, F., Hassouna, M., Hénault, C., Jeuffroy, M., Klumpp, K., Metay, A., Moran, D., Recous, S., Samson, E., Savini, I., Pardon, L., 2013. How can French agriculture contribute to reducing greenhouse gas emissions? Abatement potential and cost of ten technical measures. Synopsis of the Study Report, INRA (France).
Philippot, L., Čuhel, J., Saby, N.P.A., Chèneby, D., Chroňáková, A., Bru, D., Arrouays, D., Martin-Laurent, F., Šimek, M., 2009. Mapping field-scale spatial patterns of size and activity of the denitrifier community. Environ. Microbiol. 11, 1518–1526.
Pinheiro, J.C., Bates, D.M., 2000. Mixed-Effects Models in S and S-PLUS. Springer Science & Business Media.
Pinheiro, J., Bates, D., DebRoy, S., Sarkar, D., R Development Core Team, 2013. NLME: Linear and Nonlinear Mixed Effects Models. R Package Version 3.1-111.
Poeplau, C., Don, A., 2015. Carbon sequestration in agricultural soils via cultivation of cover crops — a meta-analysis. Agric. Ecosyst. Environ. 200, 33–41.
Power, A.G., 2010. Ecosystem services and agriculture: tradeoffs and synergies. Philos. Trans. R. Soc. Lond. B Biol. Sci. 365, 2959–2971.
Profft, I., Mund, M., Weber, G.-E., Weller, E., Schulze, E.-D., 2009. Forest management and carbon sequestration in wood products. Eur. J. For. Res. 128, 399–413.
Puget, P., Chenu, C., Balesdent, J., 2000. Dynamics of soil organic matter associated with particle-size fractions of water-stable aggregates. Eur. J. Soil Sci. 51, 595–605.
R Development Core Team, 2013. R: A Language and Environment for Statistical Computing.
Rasse, D.P., Rumpel, C., Dignac, M.F., 2005. Is soil carbon mostly root carbon? Mechanisms for a specific stabilisation. Plant Soil 269, 341–356.
Rhoades, C.C., 1997. Single-tree influences on soil properties in agroforestry: lessons from natural forest and savanna ecosystems. Agrofor. Syst. 35, 71–94.
Ribeiro, P.J., Diggle, P.J., 2001. geoR: a package for geostatistical analysis. R-News 1, 15–18.
Schroth, G., da Fonseca, G.A.B., Harvey, C.A., Gascon, C., Vasconcelos, H.L., Izac, A.-M.N., 2004. Agroforestry and Biodiversity Conservation in Tropical Landscapes. Island Press, Washington, DC.
Sharrow, S.H., Ismail, S., 2004. Carbon and nitrogen storage in agroforests, tree plantations, and pastures in western Oregon, USA. Agrofor. Syst. 60, 123–130.
Six, J., Elliott, E.T., Paustian, K., 2000. Soil macroaggregate turnover and microaggregate formation: a mechanism for C sequestration under no-tillage agriculture. Soil Biol. Biochem. 32, 2099–2103.
Somarriba, E., 1992. Revisiting the past: an essay on agroforestry definition. Agrofor. Syst. 19, 233–240.
Somarriba, E., Cerda, R., Orozco, L., Cifuentes, M., Dávila, H., Espin, T., Mavisoy, H., Ávila, G., Alvarado, E., Poveda, V., Astorga, C., Say, E., Deheuvels, O., 2013. Carbon stocks and cocoa yields in agroforestry systems of Central America. Agric. Ecosyst. Environ. 173, 46–57.
Soussana, J.-F., Loiseau, P., Vuichard, N., Ceschia, E., Balesdent, J., Chevallier, T., Arrouays, D., 2004. Carbon cycling and sequestration opportunities in temperate grasslands. Soil Use Manag. 20, 219–230.
Stavi, I., Lal, R., 2013. Agroforestry and biochar to offset climate change: a review. Agron. Sustain. Dev. 33, 81–96.
Stevens, A., Nocita, M., Tóth, G., Montanarella, L., van Wesemael, B., 2013. Prediction of soil organic carbon at the European scale by visible and near infrared reflectance spectroscopy. PLoS One 8, 1–13.
Takimoto, A., Nair, V.D., Nair, P.K.R., 2008. Contribution of trees to soil carbon sequestration under agroforestry systems in the West African Sahel. Agrofor. Syst. 76, 11–25.
Tan, Z., Lal, R., Owens, L., Izaurralde, R., 2007. Distribution of light and heavy fractions of soil organic carbon as related to land use and tillage practice. Soil Tillage Res. 92, 53–59.
Teck, R.M., Hilt, D.E., 1991. Individual-Tree Diameter Growth Model for the Northeastern United States. Res. Pap. NE-649. US. Department of Agriculture, Forest Service, Northeastern Forest Experiment Station, Radnor, PA (11 pp.).
Torquebiau, E.F., 2000. A renewed perspective on agroforestry concepts and classification. Life Sci. 323, 1009–1017.
Tully, K.L., Lawrence, D., Scanlon, T.M., 2012. More trees less loss: nitrogen leaching losses decrease with increasing biomass in coffee agroforests. Agric. Ecosyst. Environ. 161, 137–144.
Upson, M.A., Burgess, P.J., 2013. Soil organic carbon and root distribution in a temperate arable agroforestry system. Plant Soil 373, 43–58.
Varah, A., Jones, H., Smith, J., Potts, S.G., 2013. Enhanced biodiversity and pollination in UK agroforestry systems. J. Sci. Food Agric. 93, 2073–2075.
Verchot, L.V., Noordwijk, M., Kandji, S., Tomich, T., Ong, C., Albrecht, A., Mackensen, J., Bantilan, C., Anupama, K.V., Palm, C., 2007. Climate change: linking adaptation and mitigation through agroforestry. Mitig. Adapt. Strateg. Glob. Chang. 12, 901–918.
Villanneau, E.J., Saby, N.P.A., Marchant, B.P., Jolivet, C.C., Boulonne, L., Caria, G., Barriuso, E., Bispo, A., Briand, O., Arrouays, D., 2011. Which persistent organic pollutants can we map in soil using a large spacing systematic soil monitoring design? A case study in Northern France. Sci. Total Environ. 409, 3719–3731.
Virto, I., Barré, P., Burlot, A., Chenu, C., 2011. Carbon input differences as the main factor explaining the variability in soil organic C storage in no-tilled compared to inversion tilled agrosystems. Biogeochemistry 108, 17–26.
von Lützow, M., Kögel-Knabner, I., Ekschmitt, K., Flessa, H., Guggenberger, G., Matzner, E., Marschner, B., 2007. SOM fractionation methods: relevance to functional pools and to stabilization mechanisms. Soil Biol. Biochem. 39, 2183–2207.
Webster, R., McBratney, A.B., 1989. On the Akaike Information Criterion for choosing models for variograms of soil properties. J. Soil Sci. 40, 493–496.
Webster, R., Oliver, M.A., 2007. Geostatistics for Environmental Scientists.
Wiesmeier, M., Hübner, R., Spörlein, P., Geuß, U., Hangen, E., Reischl, A., Schilling, B., von Lützow, M., Kögel-Knabner, I., 2014. Carbon sequestration potential of soils in southeast Germany derived from stable soil organic carbon saturation. Glob. Change Biol. 20, 653–665.
Young, A., 1997. Agroforestry for Soil Management. second ed. CAB International, Wallingford, UK.